6. PROBING THE HARD SEGMENT PHASE CONNECTIVITY AND PERCOLATION IN MODEL SEGMENTED POLYURETHANEUREA COPOLYMERS

6.1 CHAPTER SUMMARY

Model segmented oligomeric polyurethaneureas (PUU) with or without hard segment (HS) branching were utilized to explore the importance of hydrogen bonding and HS chain architecture in mediating the long-range connectivity of the HS phase. The HS content of all the PUU materials was *ca.* 22 wt % and the soft segment was a heterofed random copolymer of 50:50 ethylene oxide: propylene oxide based mono functional alcohol of MW 970 g/mol. The role played by hydrogen bonding was investigated by incorporating varying amounts of LiCl into the PUU system *without* HS branching. While the HS phase of the linear PUU sample was based on water and an isomeric mixture of 80:20 2,4:2,6 toluene diisocyanate (TDI), a mixture of TDI and triphenylmethane-4,4',4" triisocyanate (along with water) was utilized during the chain extension step of the synthesis to incorporate HS branching. DSC and/or SAXS results on the final films indicated that the samples were still able to establish a microphase morphology even in the presence of the highest amount of LiCl (1.5 wt %) or the highest extent of HS branching utilized in the study. Tapping-mode AFM phase images of the PUU sample without LiCl or HS branching showed the presence of long ribbon-like hard domains that percolated through the soft matrix. The long-range connectivity of the HS phase was disrupted with increasing amounts of LiCl or HS branching. Accompanying such disruption was a systematic mechanical softening of the PUU samples. FT-IR indicated that addition of LiCl or incorporation of HS branching disrupted the hydrogen bonded network within the HS phase. These results indicate the importance of hydrogen bonding and chain architecture in mediating the long-range connectivity of the HS phase and achieving dimensional stability.

6.2 INTRODUCTION

Flexible polyurethaneurea (PUU) foams posses a complex morphology consisting of two coexisting networks – a covalent cross-linked network generated as a result of a tri or higher functional polyol precursor, and a physical cross-linked network formed by the association of hard segments (HS) into hard domains that become dispersed in a soft matrix. Indeed, to the authors' knowledge aside from cross-linked polyethylene, very few other commercial polymer based products possess a morphology that consists of coexisting covalent and physical cross-linked networks. The morphology of PUU foam samples with a sufficient HS size and content is characterized by a broad range of size scales, from a 3-5 nm long hard domain to a *ca.* 300 nm diameter hard segment dominated aggregate, known as a 'urea ball'. Furthermore, the dimensions of a typical single foam cell in slabstock or molded PUU foams are at least three orders of magnitude larger than the size of a urea ball.

Both the interlocking covalent and physical cross-linked networks impart structural stability to the foam matrix [1,2]. As compared to the latter, one expects the stronger covalent network to play a dominant role in imparting structural stability to the foam matrix. Elwell *et al.* [3,4] have examined the reaction kinetics and morphology development in model flexible PUU foams based on polyols and also oligomeric mono-alcohols (commonly known as *monols*). Recent efforts by Aneja *et al.* [5-7] have been also directed at gaining a fundamental understanding of the physical cross-linked network's contribution towards achieving structural stability (solidification) in materials based on related PUU chemistry. Model PUU plaques were prepared [5] by the synthesis route shown in Scheme 6.1. The PUU plaques produced were copolymers based on formulations similar to PUU foams but in which no surfactants were utilized and the released CO_2 was allowed to escape. Furthermore, the formation of a cellular structure was prevented by the application of high pressure. Utilization of a monol instead of a tri-functional polyol prevents the formation of covalent cross-links and also results in end-capping of the HS. Moreover, the MW of the resulting trisegment species is limited to less than 3000 g/mol – a moiety that would not be expected to display any significant molecular entanglement, if any at all. Thus, the investigation of only the physical cross-linked network's influence on the structural stability of the resultant plaque is possible. The HS content of the model plaques ranged from 2 parts per hundred parts polyol (pphp) water (equivalent to 22 wt % HS) to 6 pphp water (38 wt % HS)

Remarkably, s*olidification* of the PUU plaques, starting from the 22 wt % HS content sample, was observed in the same study at room temperature despite – 1) the oligomeric MW (< 3000 g/mol) of the constituent chains, 2) a lack of a covalent cross-linked network, and 3) the two end blocks of the trisegments being well above their T_g at room temperature (see later discussion).

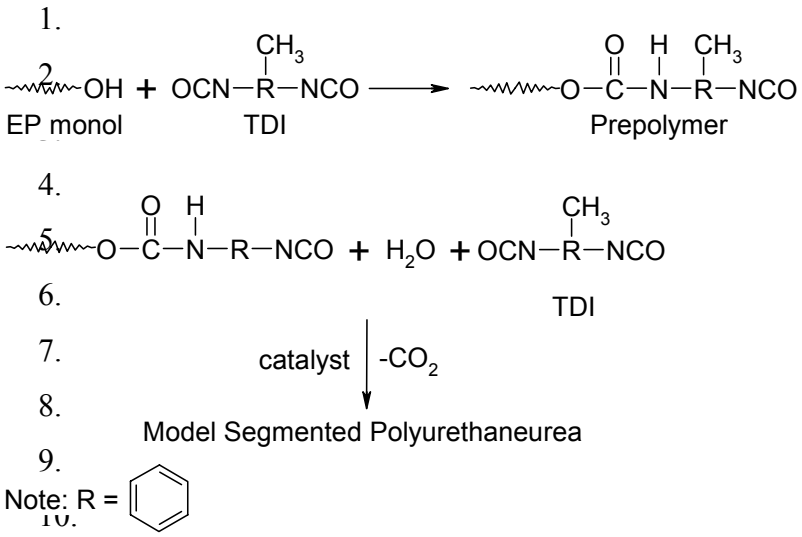

Scheme 6.1 [Adapted from Ref. 5]

The PUU plaques possessed a microphase separated morphology as determined by differential scanning calorimetry (DSC) and small angle x-ray scattering (SAXS). Indeed, tapping-mode atomic force microscopy (AFM) phase image of the 22 wt % HS content PUU plaque sample provided the first visual representation of the long-range connectivity of the HS into long ribbon-like hard domains that percolated through the soft matrix in such a low MW segmented copolymer [5]; see Section 6.3.2 for further details.

As noted earlier, the microphase separation in these PUU plaque systems is thermodynamically driven, specifically by the product χN. However, the ability of the HS to form strong secondary interactions, namely hydrogen bonding, modifies and complicates χ, thereby making the microphase separation phenomenon less predicable. The hydrogen bonding capability of the HS thus influences their association into hard domains and also the consequent microphase separation process. The question therefore that arises is, "how important is the *extent of hydrogen bonding* in mediating the long-range connectivity of the hard phase that was shown to exist in the model PUU plaques described above?" The effect

of LiCl and LiBr additives on flexible PUU foam morphology has been previously reported [6,7]. It was shown that LiCl as well as LiBr preferentially interact with the urea HS. Thus, if LiCl can systematically mediate the extent of hydrogen bonding within the urea hard domains, it can be used as a molecular probe to investigate the influence of hydrogen bonding on the long-range connectivity of the hard domains in PUU copolymers. The results of this study based on the above hypothesis are presented in Section 6.3. In particular, the concentration of LiCl in a 22 wt % HS content based PUU plaque is systematically varied to study the resulting morphology and structural stability of the model PUU plaque.

Another question that also arises is, "how does chain architecture influence the HS connectivity as well as the hydrogen bonding capability of the HS phase?" The results from an investigation which probes the role of chain architecture, specifically HS branching, in mediating the long-range connectivity of the HS and the hydrogen bonded network within the hard phase in the model segmented PUU copolymer addressed above are also presented in this chapter. Varying extents of HS branching are incorporated by utilizing different relative ratios of a di- and triisocyanate along with water during the chain extension step of the synthesis. The results of this study are discussed in Section 6.4.

6.3 USE OF LITHIUM CHLORIDE AS MOLECULAR PROBE

6.3.1 Experimental

6.3.1.1 Sample Preparation

A 22 wt % HS PUU plaque synthesized in [5] by the reaction procedure shown in Scheme 6.1 was utilized throughout the study that utilizes LiCl. Measured quantities of the model plaque were dissolved in *N*,*N*-dimethylacetamide (DMAc) to yield 20 wt % solutions. Anhydrous LiCl dissolved in DMAc was then added to the PUU plaque solutions to obtain three moisture free solution samples with 0.1, 1.0, and 1.5 wt % LiCl respectively. A fourth sample solution with no LiCl was used as a control. It may be noted that 0.1 and 1.5 wt % LiCl corresponds to an average of 1 LiCl molecule per 40 and 2.7 urea linkages respectively.

Tapping-mode AFM, FT-IR, DSC, and thermomechanical analysis (TMA) were applied as characterization tools. For AFM imaging, thin film samples on microscope glass

slides were obtained by taking a small quantity of the sample solution on a slide and allowing the solvent to evaporate in an oven at 60°C for two hours; thereafter overnight at room temperature under vacuum. A similar procedure was used to obtain thin sample films on KBr disks instead of glass slides for FT-IR. The solvent was completely evaporated from measured quantities of the four sample solutions to obtain 15-20 mg samples for the DSC experiments. A similar procedure was employed to obtain samples for TMA. All solutions and films obtained were optically clear. Due to the hygroscopic nature of LiCl, all samples were stored in a vacuum desiccator until investigated further.

6.3.1.2 Experimental Methods

Tapping-mode phase AFM of the free surface of solution cast films was conducted via a Veeco Dimension 3000 scanning probe microscope using Nanosensors' TESP 7 tips. 2 μm x 2 μm images were captured at a set-point ratio of *ca.* 0.6. Further instrumentation details can be found in Section 3.3.2.

FT-IR in transmission mode was conducted in a Nicolet 510 spectrometer. Spectra of films on KBr disks were collected at a resolution of 2 cm^{-1} and 64 scans were co-added to each file. A background, 64 scans at a 2 cm^{-1} resolution, was collected before each sample run.

A Seiko DSC 220C was used to subject thoroughly dried samples to a heating scan from -100°C to 25°C at the rate of 10°C/min under a dry nitrogen atmosphere.

TMA experiments were conducted at room temperature in a Perkin Elmer DMA 7e by following the penetration of a rounded conical quartz probe in to the sample for a period of 10 minutes. A constant load of 3 mN was applied during the experiment.

6.3.2 Results and Discussion

The tapping-mode AFM phase image of the 22 wt % HS content based PUU plaque sample cast on a glass slide directly from the reaction mixture was presented in Ref. 5. It is reproduced here as Fig. 6.1 for the sake of comparison of its morphology with that of a solution cast sample, whose AFM image is presented in Fig. 6.2a. The AFM image in Fig. 6.1 shows percolation of thin, ribbon-like hard domains dispersed in the soft monol based

matrix. As noted in the earlier discussion, this plaque was a distinct brittle solid, i.e. when the reaction mixture was cast in a 'picture-frame' mold and annealed under pressure at 100°C for 2 hours a brittle, rigid, and self-supporting solid was obtained. Thus, this AFM phase image provided direct evidence that long-range connectivity of the HS plays an important role in promoting cohesive strength and dimensional stability that accompanies a transformation from the liquid to a solid state. Such percolation of the hard domains was possible due to the fact that in the absence of surfactants and covalent cross-links (which typically results in commercial PUU foam chemistry), and the viscosity build-up, which usually accompanies the overall MW build-up in a sample, was not as rapid. Hence individual urea based HS were able to associate more easily as promoted by hydrogen bonding and were able to aggregate into ordered ribbon-like hard domains with long-range connectivity. The presence of a microphase separated morphology was also confirmed by SAXS and DSC. A broad first order interference peak with an inter-domain spacing of *ca.* 115Å was seen in the SAXS profile. Such a '*d'* spacing is consistent with the general spacing seen between the ribbon-like hard domains in Fig. 6.1. A soft phase T_g of *ca.* -63°C in the PUU plaques was observed via DSC. As expected, it was higher than the pure monol T_g (-76°C) due to the soft segments' restricted mobility, which is affected by their covalent 'tethering' with the HS and also possibly due to some potential microphase mixing.

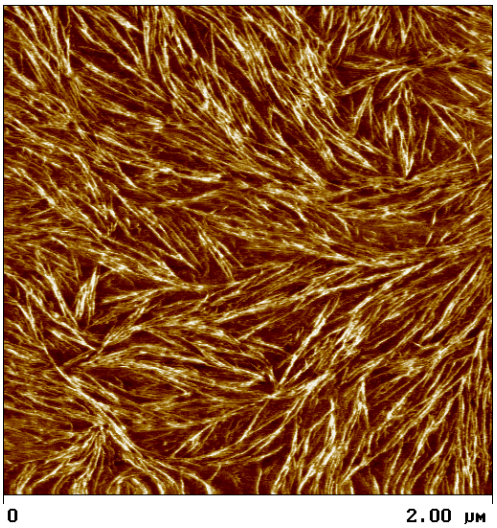

Figure 6.1 Tapping-mode AFM phase image of 22 wt % HS content based model PUU plaque [Reproduced from Ref. 5].

An AFM phase image of a solution cast 22 wt % HS content based PUU film is presented in Fig. 6.2a. The overall morphology of the solution cast sample is similar to that exhibited by the sample cast directly from the reaction mixture (Fig. 6.1). However, in this instance one also notes that the ribbon-like hard domains exhibit packing somewhat similar to that exhibited by some nematic liquid crystals [8]. In fact, a disclination-like 'wall' defect in the packing topology is seen near the center of the phase image where a portion of the ribbons has 'turned' so as to improve the degree of packing (see arrow). Also presented in Fig. 6.2 are AFM phase images of solution cast 22 wt % HS content based PUU samples with 0.1, 1.0, and 1.5 wt % LiCl respectively. It may be recalled that 0.1 and 1.5 wt % LiCl corresponds to an average of 1 LiCl molecule per 40 and 2.7 urea linkages respectively. At 0.1 wt % LiCl loading (Fig. 6.2b), one notes no noticeable disruption in the long-range connectivity of the hard domains. However, when the LiCl concentration is increased by an order of magnitude, to 1.0 wt % (Fig. 6.2c), there is a substantial breakdown of the long-range connectivity of the hard domains and only short rod-like hard domains survive. The percolation of the HS is seen to be almost completely destroyed at 1.5 wt % LiCl concentration (Fig. 6.2d).

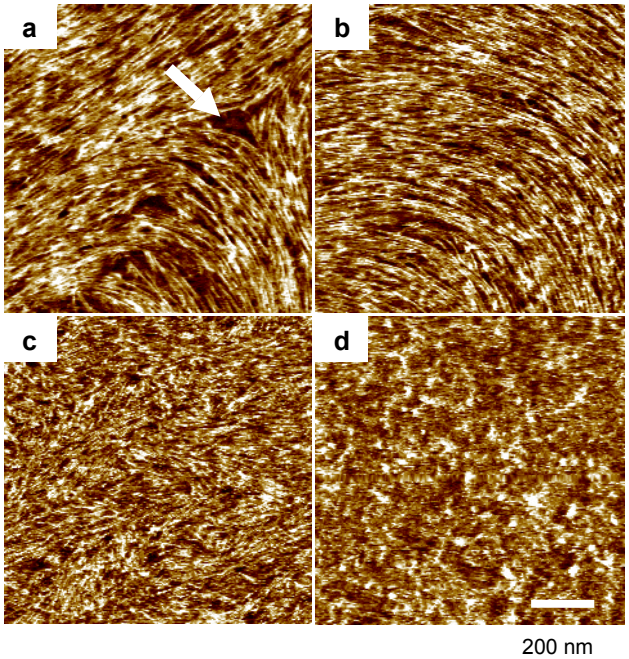

Figure 6.2 Tapping-mode AFM phase images of solution cast oligomeric trisegment PUU films with (a) 0.0; (b) 0.1; (c) 1.0; and (d) 1.5 wt % LiCl.

Furthermore, the systematic disruption of the long-range connectivity of the hard domains by LiCl resulted in a *systematic softening* of the samples as confirmed by penetration-mode TMA. From Fig. 6.3, it is noted that over the same time period (10 min), the depth of the TMA probe penetration increases with increasing LiCl content of the sample.

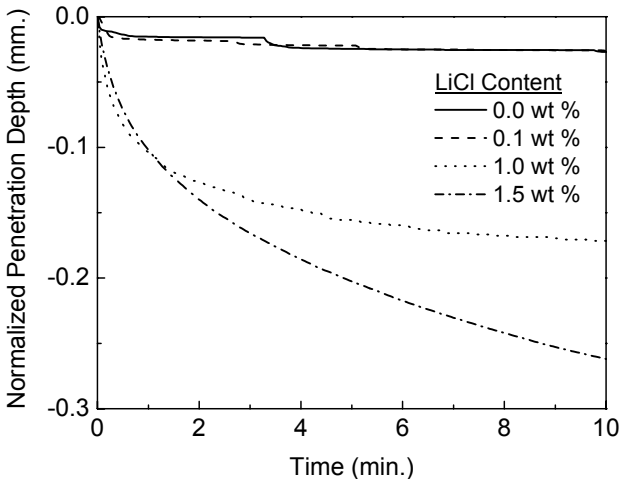

Figure 6.3 TMA probe penetration in 22 wt % HS content based solution cast oligomeric trisegment PUU films with LiCl.

DSC heating scans of solution cast 22 wt % HS content based PUU sample, with 0.0, 1.0 and 1.5 wt % LiCl respectively are presented in Fig. 6.4. The PUU sample without any LiCl exhibits a soft segment T_g of *ca.* -63°C, which is similar to that of the 22 wt % HS content based PUU plaque as noted previously. This indicates that the solution cast sample distinctly possesses a microphase separated morphology. The shift of its T_g to a higher temperature as compared to that of the pure monol no doubt arises, as mentioned earlier, due to the restricted mobility of each of the two soft segments at the one end at which they are covalently linked to TDI via a urethane linkage and also limited extent of microphase mixing. The solution cast 22 wt % HS content based PUU sample with 1.0 wt % LiCl shows at best only a very small increase in its soft segment T_g at -62°C. The similar T_g indicates that the degree of microphase mixing is still nearly the same as that of the material with no LiCl. Such a result is consistent with the AFM phase image (Fig. 6.2c) of this sample. Interestingly, even the sample with 1.5 wt % LiCl retains microphase separation, as indicated by its soft segment T_g of -61°C. Thus, from the thermal analysis it is noted that all the solution cast samples are able to maintain a microphase separated morphology, even when

the concentration of LiCl in the sample is as high as 1.5 wt %. It may be noted that the HS T_g could not be observed from the DSC heating profiles of the four samples due to the very small heat capacity change in their glass transition. The difficulty of observing the T_g of the HS phase in segmented PUU is widely known in the literature [9,10].

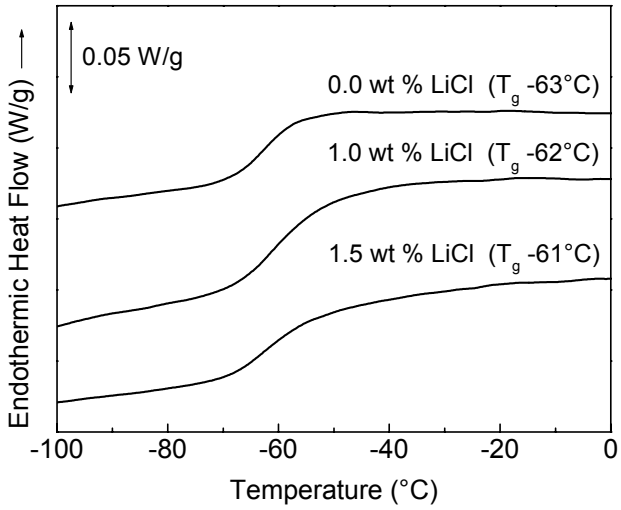

Figure 6.4 DSC heating scans of 22 wt % HS content based solution cast oligomeric trisegment PUU films with LiCl.

After confirming the ability of LiCl to interact with the model PUU plaque, it becomes important to examine the nature of this interaction. FT-IR can be used to elucidate such a phenomenon. In the IR region between 1700 and 1600cm^{-1}, the urea carbonyl (C=O) group can exhibit two absorbance peaks; at 1680 and 1640 cm^{-1} corresponding to free and hydrogen bonded C=O respectively [3,11]. The intensity of these peaks can be used to measure the relative concentration of free and hydrogen bonded C=O groups. The FT-IR spectra are presented in Fig. 6.5. It may be noted that the absorbance peak at 1600 cm^{-1} corresponding to the in-plane vibration in the aromatic ring of TDI in the PUU plaque sample with no LiCl was used as a reference and baseline corrections were applied to all the absorbance spectra. From Fig. 6.5, it is noted that as the amount of LiCl in a given sample increases, there is a systematic decrease in the absorbance intensity of the hydrogen bonded urea C=O (1640 cm^{-1}) peak with a corresponding increase in the intensity of the free C=O (1680 cm^{-1}). Within the ether absorbance region, between 1200 and 1000 cm^{-1}, no significant change in the absorbance intensity of the peak at *ca.* 1110cm^{-1} was noted. LiCl has been

shown [6] to similarly interact preferentially with the hard domains of flexible slabstock PUU foams and their plaque counterparts.

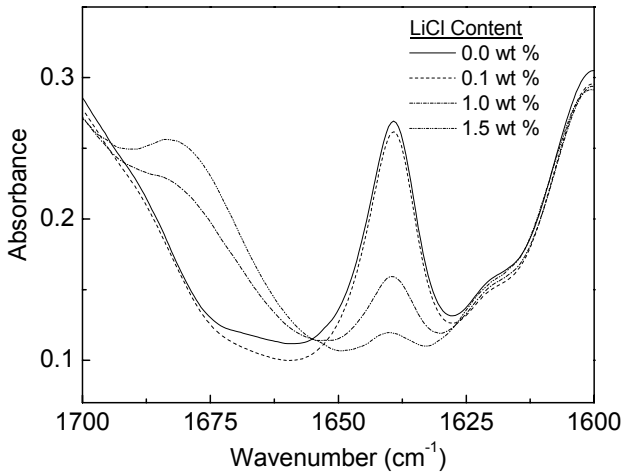

Figure 6.5 Urea C=O stretching region of the FT-IR spectra of 22 wt % HS content based solution cast oligomeric trisegment PUU films.

Thus FT-IR provides very strong support to the visual observations made via AFM regarding the ability of LiCl to interact with the hard domains of these model PUU samples. In effect, LiCl limits the ability of the HS to form hydrogen bonds. Thus, a reduced extent of hydrogen bonding within the hard domains results in a disruption of long-range order and the loss of the percolated hard phase. Consequently, as the LiCl content increases the sample begins to lose dimensional stability and softens.

A highly simplified schematic representation of the interaction of LiCl with the HS is presented in Fig. 6.6, which is based on the results generated by AFM, DSC and FT-IR. Depicted in Fig. 6.6a is the ordered packing of the HS into hard domains. Also presented in Fig. 6.6a is the ability of the HS to form a regular hydrogen-bonded network. The nature of the interaction of LiCl with the HS and the consequent disruption of some of the hydrogen bonds within the hard domains of a model PUU sample is depicted in Fig. 6.6b. It is recognized that for small molecules that undergo hydrogen bonding (eg. water) they create a very 'dynamic' network wherein individual bonds continuously break and reform due to Brownian motion of the small moieties [12]. However, in the present case the HS in these oligomeric materials exist below their T_g at room temperature. Hence, their hydrogen bonded

network is expected to be much less mobile or dynamic. Therefore the depiction of this network in Fig. 6.6 as made up of 'equilibrium' interactions is not wholly unrealistic.

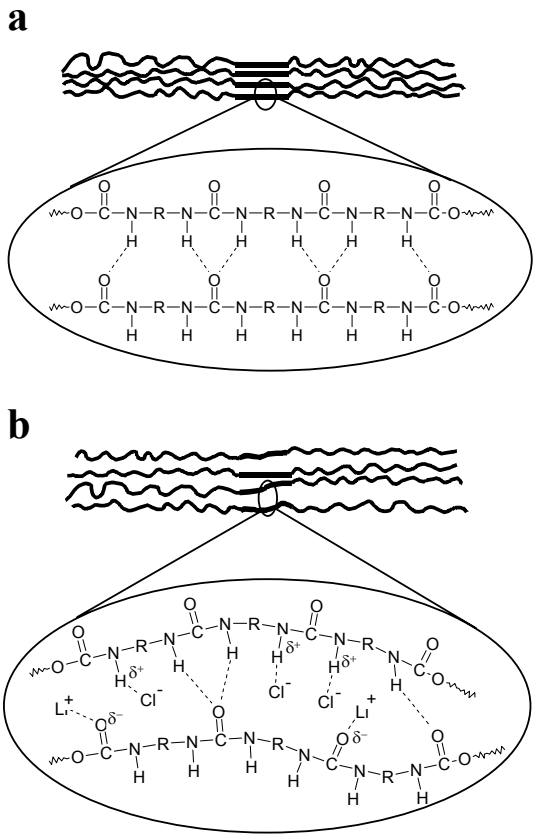

Figure 6.6 Simplified schematic representation of the model trisegment oligomeric PUU without LiCl (a); and with LiCl (b).

6.4 INCORPORATION OF HARD SEGMENT BRANCHING

6.4.1 Experimental Section

6.4.1.1 Materials

A heterofed 50:50 ethylene oxide and propylene oxide based mono functional alcohol of MW 970 g/mol, a 80:20 isomeric mixture of 2,4:2,6 toluene diisocyanate (TDI), a

triphenylmethane-4,4',4" triisocyanate (TTI) and deionised water were used as raw materials along with a conventional catalyst package consisting of 5:1 parts by weight of Dabco 33LV:BL11. Bayer Chemicals graciously supplied the EP monol, and the diisocyanates, TDI and TTI. These precursors were utilized without further purification. Air Products kindly provided the Dabco catalyst package.

6.4.1.2 Synthesis

The synthesis scheme [13] utilized to produce model segmented PUU copolymers with HS branching is presented in Scheme 6.2. This route is similar to the one described in Scheme 6.1 but with one difference, which is discussed below.

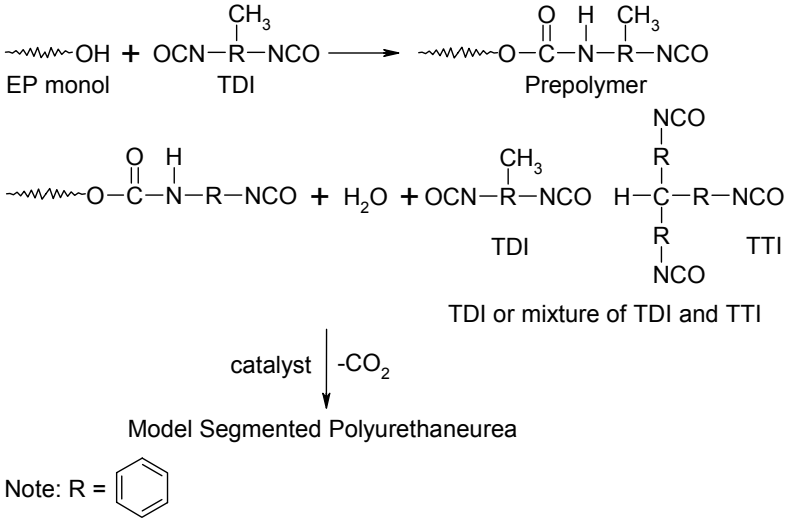

Scheme 6.2

To synthesize the prepolymer, 485 g of the EP monol followed by 87 g of TDI were added to a 1 L flame dried round bottom flask. After the addition of the reactants the mixture was stirred vigorously for 30 minutes and thereafter placed in an oven at 60°C for 24 hours to ensure completion of the reaction. The prepolymer was then allowed to cool to ambient temperature. Small quantities of this prepolymer (*ca.* 28 g) were then chain extended with deionised water and a mixture of a di (TDI)-functional and tri (TTI)-functional isocyanate. Different ratios of TDI/TTI were utilized to synthesize a total of five segmented PUU with varying extents of HS branching but a fixed HS content of 22 wt %. The chain extension step

was catalyzed with less then 0.2 wt % of the Dabco catalyst package. The reader may recognize that the above synthesis route mimics PUU foam chemistry except that in the present instance no surfactants are utilized and the tri or higher functional polyol is replaced with a monol. Such a route was adopted in light of the longstanding interest of Prof. Wilkes' laboratory in the structure-property behavior of water blown flexible PUU foams [1,14-17]. Generally, in the production of these materials, the reaction of water with an isocyanate results in the evolution of carbon dioxide, which is utilized as an 'in situ' foaming agent. However, in the present study, the reaction mixtures were stirred continuously until the evolution of CO_2 ceased. Each of the resulting segmented PUUs were poured into a 'picture-frame' mold and sandwiched between Teflon sheets and steel plates. This assembly was then placed in a hot-press at 100°C and under 10,000 kg_f for 2 hours to ensure completion of the reaction. The resulting solid plaques were stored under vacuum at ambient temperature until used for analysis. The TTI content (and therefore the extent of HS branching) in the copolymers was 0.14, 0.60, 0.80, 1.60, and 2.90 wt % respectively. It may be noted that 0.14 and 2.9 wt % TTI correspond to replacing 1 % and 25 % of the TDI-NCO groups with TTI-NCO groups respectively in the chain extension step of the synthesis. A linear trisegment PUU with 22 wt % HS content, which was synthesized by chain extending the prepolymer with deionised water and TDI alone was used as a control. Following their polymerization, all six samples were completely soluble in dimethyl acetamide indicating the absence of any gel formation.

6.4.1.3 Experimental Methods

AFM, DSC, WAXS, and TGA were conducted by using the equipment and procedure described above in Section 6.3.1.2 with one exception. A constant load of 30 mN was applied on the samples during the TGA experiments instead of 3 mN that was utilized earlier. The SAXS profiles were collected according to the procedure described in Section 3.3.2.

6.4.2 Results and Discussion

Tapping-mode AFM phase images of solid PUU plaques with 22 wt % HS content but varying extents of HS branching are presented in Fig. 6.8. In these phase images, by

convention, the hard and soft microphases appear as bright and dark regions respectively. The linear trisegment PUU (Fig. 6.2a) exhibits long ribbon-like hard domains, which percolate through the soft matrix. Upon comparison of the two phase images in Figs. 6.2a and 6.7a it is noted that both the solution cast film and the solid plaque respectively posses similar morphologies. Besides the percolated ribbon-like hard domains, a common morphological feature in their respective packing topology is the presence of wall or disclination-like defect where the ribbons have 'turned' to allow for continuation of packing. As noted earlier such an extensively percolated hard phase reinforces the soft matrix and enables the oligomeric sample to solidify into a relatively rigid system. Such morphology also suggests that the HS pack orthogonally to the long axis of the ribbons. A similar packing has also been noted in polytetramethylene oxide based polyurethanes and polyureas with uniform length HS [18,19] or poly(ether ester aramides), also with uniform length HS [20].

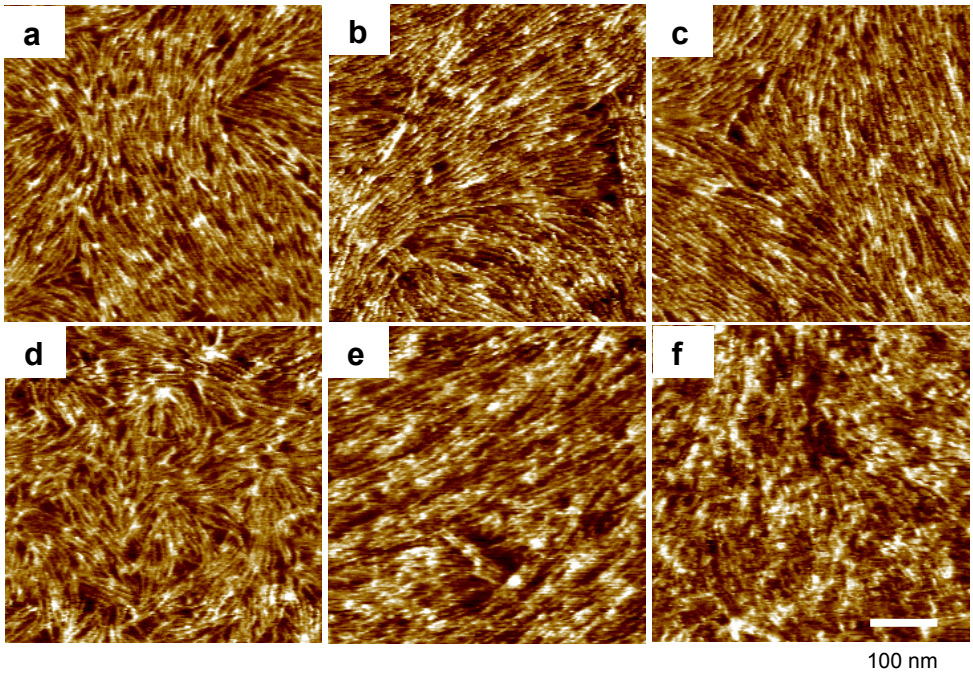

Figure 6.7 Tapping-mode AFM phase images of model segmented PUU solid plaques containing (a) no TTI, this sample is a linear trisegment PUU with overall MW < 3000 g/mol; (b) 0.14; (c) 0.6; (d) 0.8; (e) 1.6; and (f) 2.90 wt % TTI.

The incorporation of HS branching, up to 1.6 wt % TTI (Fig. 2e), does not result in any apparent large scale disruption of the HS long-range connectivity. However, the limited break-up of the ribbons may result in a broadening in the size distribution of the hard

domains. At a TTI loading of 2.6 wt % (Fig. 2f) one is still able to note the presence of bright and dark regions that indicate the presence of a microphase morphology. However, the ribbon-like hard domains cannot be clearly discerned, which suggests that incorporation of HS branching makes it increasingly difficult for the HS to pack efficiently and percolate through the soft matrix. In fact, the extent of HS branching enabled by the incorporation of 4.6 wt % TTI hinders HS packing to such an extent that this sample is unable to solidify and it remains a viscous liquid. While the disruption of the long-range connectivity of the HS phase upon addition of HS branching is distinct, it is not as striking as was noted earlier for the addition of LiCl to the fully TDI-based system (recall Fig. 6.2).

The direct consequence of the incorporation of HS branching is the systematic softening of the samples as confirmed by TMA. From Fig. 6.8 it is noted that the extent of the probe penetration over a period of 10 minutes increases with increasing TTI content of the sample. The rate of penetration of the probe slows considerably after 2 minutes, because the incorporation of HS branching also raises the overall MW of the sample. This results in an increase in the viscosity of the copolymer, which may partially counterbalance the softening of the sample that would occur due to the loss in HS percolation.

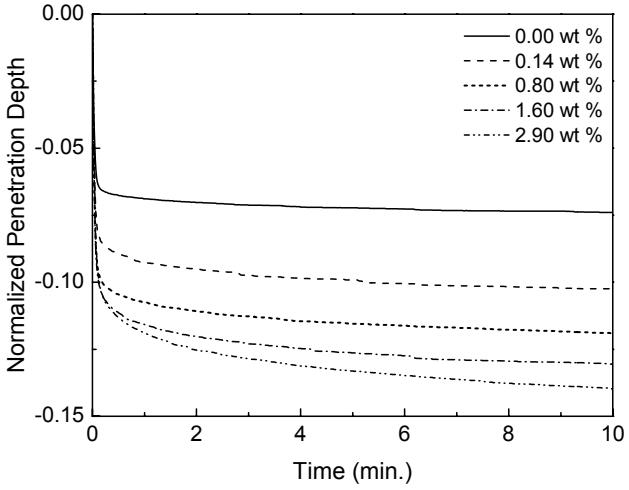

Figure 6.8 TMA probe penetration in model segmented PUU solid plaques containing varying extents of HS branching.

On the other hand, the results of the earlier study (recall Fig. 6.3) demonstrated that the addition of different amounts of LiCl into the linear trisegment based PUU did not affect the overall MW of the copolymers. Thus, in that study, the systematic softening of thoroughly dried samples with increasing LiCl content was more pronounced and the rate of the TMA

probe penetration over a period of 10 minutes was also greater than that noted in the present study.

The microphase morphology of the copolymers addressed in this study was further probed by utilizing SAXS, which is a bulk technique. The slit-smeared SAXS profiles of the six segmented PUU copolymers are presented in Fig. 6.9. As can be observed in Fig. 6.9a, the samples with up to 0.8 wt % TTI content clearly exhibit a shoulder in their respective scattering profiles. These samples exhibit an interdomain spacing or a *d* spacing, which estimated by Bragg's law is the inverse of the scattering vector *s*, of *ca.* 80Å. The first order interference shoulder in the scattering profiles of the copolymers with 1.60 and 2.90 wt % TTI (Fig. 6.9b) is distinctly less defined than in the samples with lower TTI content.

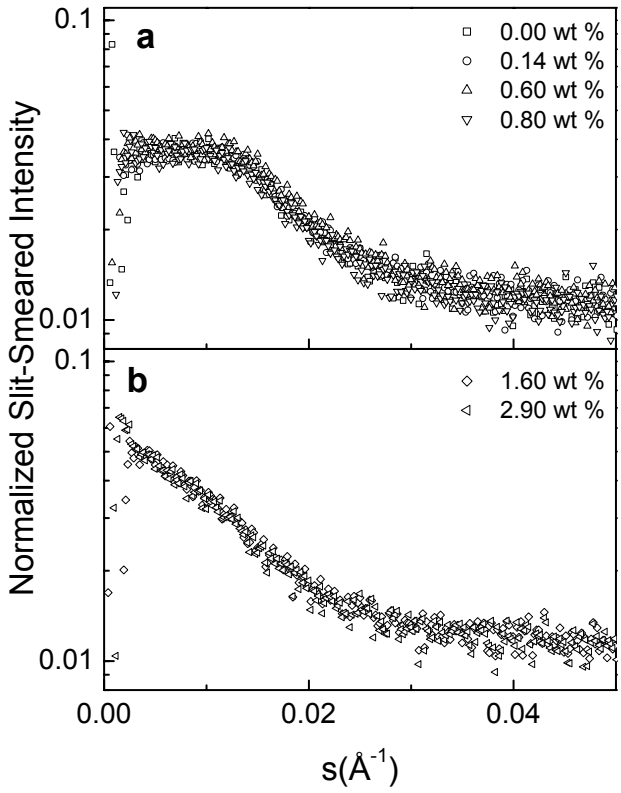

Figure 6.9 Slit-smeared SAXS profiles of model segmented PUU solid plaques (a) the intensity of profiles of samples with 0.00, 0.15, 0.60, and 0.80 wt % TTI, (b) the intensity of profiles of samples with 1.60 and 2.90 wt % TTI.

In light of the similar SS T_g of all six copolymers as observed by DSC (Fig. 6.10), the SAXS response of the two samples with 1.60 and 2.90 wt % TTI respectively suggests that HS branching possibly leads to a broader distribution of the hard domain sizes. In fact, the

reader may recall that such behavior was also noted in the respective AFM phase images (Figs. 6.7e and f) of these two samples. Thus, both AFM and SAXS results are consistent with each other.

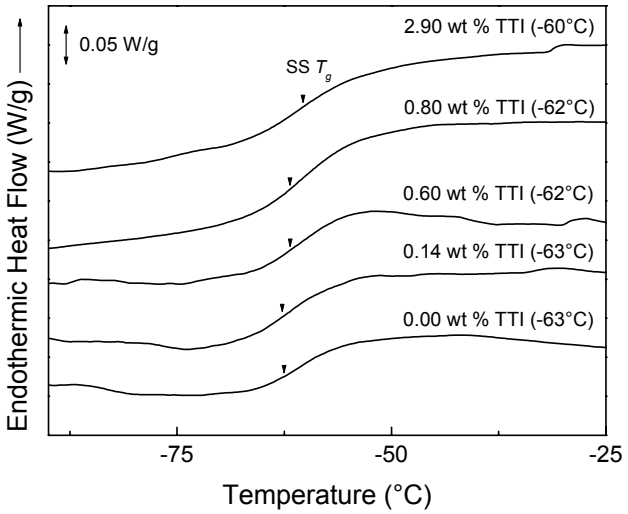

Figure 6.10 DSC profiles of selected model segmented PUU solid plaques. A given sample's T_g is given in rounded brackets next to its TTI content. Note that any HS T_g in the six copolymers' DSC heating profiles was not observed due to the small heat capacity change exhibited by this phase during its glass transition.

So far it has been demonstrated by utilizing the techniques of AFM and SAXS that the incorporation of HS branching in the model segmented PUU addressed in this study results in the disruption of the HS's long-range connectivity, which in turn leads to a systematic softening of the samples as confirmed by TMA. The impact of HS branching on the state of the hydrogen bonded network in these model PUU was also investigated by FT-IR. As noted earlier, in the IR region between 1700 and 1600 cm^{-1}, the urea carbonyl (C=O) group can exhibit two absorbance peaks; at 1680 and 1640 cm^{-1} corresponding to free and hydrogen bonded C=O respectively. The intensity of these peaks can be used to measure the relative concentration of free and hydrogen bonded C=O groups. Earlier it was noted that the intensity of the bonded peak at 1640 cm^{-1} decreases systematically with increasing LiCl content and as expected, it is accompanied by a corresponding increase in the intensity of the 1680 cm^{-1} free peak (see Fig. 6.5). Thus, in this earlier work, FT-IR demonstrated that such a disruption of the hydrogen bonded network by addition of LiCl resulted in the loss of the long-range connectivity of the HS phase. In the present case, it is noted from Fig. 6.11 that as

the TTI content (or HS branching) of the copolymer increases the absorbance intensity of the urea bonded peak (1640 cm^{-1}) decreases. Surprisingly, the expected concomitant increase in the absorbance intensity of the urea free peak (1680 cm^{-1}) is not clearly evident. However, the FT-IR response of these samples in general demonstrates that as the level of HS branching increases, the ability of the HS to pack effectively and establish a hydrogen bonded network suffers.

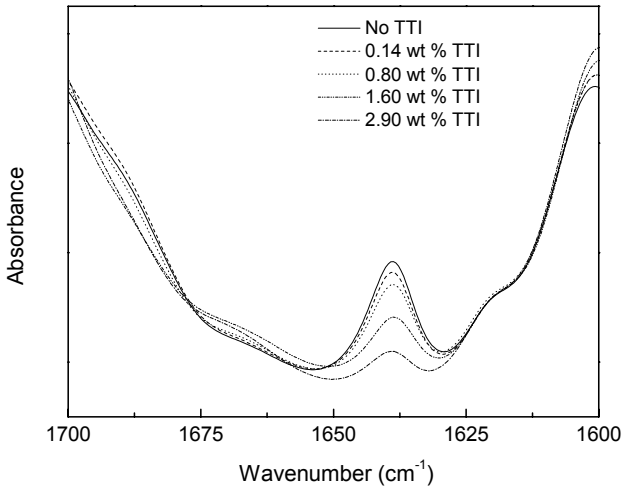

Figure 6.11 Urea C=O stretching region of the FT-IR spectra of solution cast films model segmented PUU with HS branching.

6.5 CONCLUSIONS

LiCl was used as a molecular probe to investigate the influence of the extent of hydrogen bonding on the ability of the HS to develop long-range connectivity and percolation of the hard domains through the soft polyether matrix. Samples of a model trisegment oligomeric PUU with 22 wt % HS cast from 20 wt % solutions in DMAc were used in the study. The tapping-mode AFM phase image of the model PUU without LiCl exhibited the presence of long interconnected ribbon-like hard domains that percolated through the soft monol based matrix. The AFM phase images of the solution cast samples with LiCl exhibited a systematic disruption of the hard phase connectivity as the concentration of LiCl was increased. Accompanying the disruption of the hard domain long-range connectivity was a systematic softening of the samples as confirmed by TMA. DSC demonstrated that the samples with

LiCl were able to maintain a microphase separated morphology. FT-IR experiments confirmed the ability of LiCl to interact preferentially with the urea HS and to disrupt their hydrogen bonding.

Thus, it can be concluded that over and above the presence of a microphase separated morphology, hydrogen bonding within the hard domains can be greatly beneficial in segmented PU copolymers with low degree of polymerization, in promoting additional rigidity or solidification. In the particular case of flexible PU foams, although the stronger covalent cross-link network is undoubtedly expected to play a dominant role in imparting structural stability to the material, as demonstrated in the present study, the physical cross-linked network also plays an important role towards this end.

Model segmented PUU copolymers with varying extents of HS branching were utilized to study the influence of chain architecture on the morphology of these materials. The HS branching was incorporated by utilizing a triisocyanate along with a diisocyanate and water during the chain extension step of the synthesis. The relative ratio of these two isocyanates was controlled to synthesize five copolymers with varying extents of branching but a constant HS content of 22 wt %. A linear trisegment also with 22 wt % HS content, which was synthesized by utilizing no triisocyanate during chain extension, was used as a control. The incorporation of HS branching reduced the ability of the HS to pack effectively and establish long-range connectivity. Such disruption resulted in the softening of the copolymers. While the samples were able to retain a microphase morphology in the presence of 2.90 wt % TTI as confirmed by DSC, AFM, and SAXS, the latter two techniques revealed that HS branching possibly induces a broader hard domain size distribution. HS branching also places limitations on the ability of the HS to develop a well-structured hydrogen bonded network as noted by FT-IR.

Thus, these results demonstrate that both the hydrogen bonding capability of the HS as well as the ability of the HS to establish long-range connectivity and percolation through the soft matrix are influenced by the extent of HS branching. In addition, the rigidity or stiffness of the segmented PUU addressed in this study depends upon the extent of the HS percolation through the soft matrix.